

Article

Fiber Aggregation in Nanocomposites: Aggregation Degree and Its Linear Relation with Percolation Threshold

Baorang Cui¹, Fei Pan^{2*}, Bin Ding¹, Feng Zhang¹, Yong Ma¹ and Yuli Chen^{1*}

¹ Institute of Solid Mechanics, Beihang University, Beijing 100191, China

² School of Aeronautic Science and Engineering, Beihang University, Beijing 100191, China

Abstract: Fiber aggregation in nanocomposites has an important effect on the macroscopic electrical performance. To quantitatively evaluate its effect, an index to characterize the degree of aggregation is imperative, and ideally it should have three features simultaneously, i.e., single-parametric, dimensionless and physically meaningful, applicable to different aggregation topologies, and one-to-one corresponding to material electrical properties. To this end, a new aggregation degree is proposed, which is defined as the average increased number of fibers that connect with each one when fibers aggregate from a uniformly distributed state. This index is applicable to different aggregation topologies from lump-like aggregating clusters to network-like aggregating clusters. This index is proven to only depend on the local features of aggregating clusters, and can be concisely expressed by the characteristic parameters of local structure, via geometric probability analysis and numerical validations. Further, a one-to-one linear relation between the aggregation degree and percolation threshold is established by Monte Carlo simulations, which is independent of the distribution law of the fibers. This work provides a guide to the property characterization, performance prediction and material design of nanocomposites, and also gives a physical insight into the understanding of systems with similar non-uniform distributions.

Keywords: Nanocomposites; Degree of aggregation; Analytical modelling; Percolation threshold

1. Introduction

Nanofiber reinforced composites have extensive applications in many fields, e.g. antennas and solar sails for spacecraft¹, flexible wearable electronics², high-efficiency solar cells³, highly sensitive sensors⁴, conductive coatings for lightning strike protection and electromagnetic interference shielding⁵ due to excellent physical, chemical and mechanical properties⁶, such as light weight, high specific stiffness and specific strength, high electrical/thermal conductivity, and transparency.

The spatial dispersion state of the fibers in the matrix is a core feature of composites besides the intrinsic properties of fibers, such as aspect ratio^{7,8}, curliness⁹, and plays an important role in tuning the macro properties^{10,11}. Generally, increasing the uniformity of dispersion of fibers would improve the material properties related to the connectivity of fiber network^{7,12,13}. For example, fibers with higher uniformity of dispersion are easier to construct a connecting pathway spanning through the whole materials for conducting electricity, transferring heat and carrying load, leading to a lower percolation threshold¹⁴. However, even when the dispersion state can be improved by using mechanical methods¹⁵ (e.g. sonication, ball milling and shear mixing) or chemical methods¹⁶ (e.g. surfactants and functionalization methods), re-aggregation of fillers in the subsequent processing (e.g. curing processing) may occur due to the entanglement and interaction between the fillers^{7,11,17,18}. Although aggregation could slightly facilitate local electron transfer by enhancing fiber-to-fiber contact¹⁹⁻²¹, it can reduce the global connectivity of fiber networks and thus increase

* Corresponding authors: yulicheng@buaa.edu.cn (Yuli Chen); fei_pan@buaa.edu.cn (Fei Pan)

the percolation threshold, significantly degrading the electrical property of composites^{7, 12, 22-25}. Therefore, the effect of fiber aggregation on composites properties is crucial and should be carefully treated in the process of material design and manufacturing.

Before investigating the effect of the fiber aggregation on composite properties, it is imperative to quantitatively evaluate the degree of aggregation. The microstructure of nanofiber in composites usually can be characterized by microscopies and image analysis. It is observed that the nanofibers can aggregate into lump-like clusters^{19, 26, 27} or network-like structures with the boundaries of clusters overlapped²⁸, with different fabrication techniques. When the degree of aggregation is relatively high, the aggregating clusters can be distinguished clearly in the microscopic images, and thus the degree of aggregation usually can be evaluated by the features of aggregating clusters. One of the widely used characterizing methods for the degree of aggregation is based on two indices^{17, 26}, *e.g.*, the variations of location and the size of aggregating clusters. A typical example is the quadrat method based on image processing. With a preliminary grids division of the microscopic image of composites sample, the standard deviation of the clusters' area per grid, as well as the characteristic parameter of distribution law for the size of clusters can be abstracted to describe the degree of aggregation²⁶. Most of these methods need a division of the sample image in advance. The most noticeable inconvenience of these quadrat methods is that the precision and reliability of calculation largely depend on the grid size and number of aggregating clusters^{17, 26}. Although some works have been done to remove the effect of grid size and number of aggregating clusters to obtain reliable results¹⁷, these methods should be used "with caution"^{17, 29, 30}. Additionally, it is inconvenient to evaluate the overall dispersion quality of samples when using multi-parameter model, which would lead to decision with subjectivity²⁹. Therefore, some efforts have been made by using measures with single index³¹⁻³³, which are based on statistical parameters, such as entropy^{31, 32}, and energy³³. These indices can quantitatively evaluate the degree of aggregation, but are not easy to obtain due to their complex definitions or mathematics¹⁷. When the degree of aggregation is relatively small, the nanofibers in the composites present network-like structures, where the boundaries of the aggregating clusters are hard to distinguish due to partial overlap. Therefore, the local features at the level of fibers should be considered to evaluate the degree of aggregation. To this end, some studies have employed multi-level models with the local features of fibers to investigate the electrical property of nanofiber composites, where the aggregating clusters are assumed to have the same size and distribute randomly or regularly in the matrix^{7, 11, 22, 23, 34, 35}. Based on the multi-level model, a typical evaluation for the degree of aggregation is using three indices, *i.e.*, the nominal radius of aggregating clusters, the volume fraction of nanofibers in each aggregating cluster, and the ratio of aggregated nanofibers to the total nanofibers^{7, 34}. From all the above, it can be found that evaluation for the degree of aggregation that use fewer indices and apply to different aggregation topologies still remain insufficiently explored.

Therefore, this paper aims to establish a simple and universally applicable index to quantitatively characterize the dispersion state of fibers, and further determine the relation between this index and the percolation threshold. First, a newly defined index named aggregation degree is proposed. Then, as a function of the characteristic parameters of aggregations, aggregation degree is derived analytically and validated numerically based on a two-level model with aggregated fibers. After that, a linear relation between the aggregation degree and the percolation threshold is determined by Monte Carlo simulations. Finally, a brief conclusion is summarized at the end of this paper.

2. Aggregation degree

2.1. Definition of the aggregation degree

An index for characterizing the aggregation degree of nanofiber reinforced composites should be simple, universal and easy to characterize material properties. To achieve this purpose, an ideal aggregation degree should have the following three features simultaneously.

1. The aggregation degree should be a single dimensionless index with physical meaning.
2. The aggregation degree should be applicable to different aggregation topologies from lump-like aggregating clusters to network-like aggregating clusters.
3. The aggregation degree should have a one-to-one corresponding relation with the electrical property of composites regardless of the distribution law of fibers.

To obtain an index that can have the above features and facilitate the evaluation for the effect fiber aggregation on electrical properties of composites (the percolation threshold is focused in this work), the key point is to find a parameter closely related to the dispersion state of fibers. Meanwhile, this parameter should be able to reflect the feature at the level of fiber, and thus can apply to different aggregation topologies. It is well-known that the distribution state of the fibers can be reflected by the average number of fibers that have interaction with each fiber^{36,37}, also known as average intersection number (soft core fiber) or average bond number (hard core fiber). This number can be derived from the probability of two arbitrary fibers to intersect (soft core fiber) or contact (hard core fiber) with each other. Meanwhile, for composites with uniformly distributed fibers, *i.e.* the center points of fibers distribute evenly in the space and the orientation angles of fibers follow uniform distributions in the ranges of $[0, \pi)$, the average interaction number of each fiber is a well-accepted and powerful parameter to theoretically predict the percolation threshold^{38,39}. Obviously, when the fibers cannot disperse uniformly in the matrix, the probability for two arbitrary fibers to intersect or contact with each other would change, and the average interaction number on each fiber would also change accordingly. Therefore, it is reasonable to assume that the aggregation degree is related to the variation quantity of the average interaction number, and defined as

$$\xi = \overline{N}_{\text{int}} - \overline{N}_{\text{int}}^{\text{R}}, \quad (1)$$

where $\overline{N}_{\text{int}}$ is the average interaction number of fibers with aggregation, and $\overline{N}_{\text{int}}^{\text{R}}$ is average interaction number of the same fibers with an assumed uniformly distributed state (*i.e.* without aggregation). In another word, ξ is a shifted average interaction number of fibers. It can be seen from the definition that the aggregation degree has the first feature.

According to the definition in Eq.(1), the aggregation degree of fibers is an index which represents a deviation from an assumed state when the same fibers are uniformly distributed. For fibers with uniform distribution, it equals to 0. For simplicity, the soft-core fiber model^{4,36,37,40} is employed here, where the penetration between fibers is permitted. Therefore, the fibers can intersect with each other and the average interaction number is the average intersection number. For the average intersection number of fibers with uniform distribution in 2-dimensional (2D) space, it can be obtained by geometric probability analysis³⁸, and can be expressed as

$$\overline{N}_{\text{int}}^{\text{R}} = p^{\text{R}} \cdot N_{\text{f}} = \frac{2}{\pi} \frac{l_{\text{f}}^2}{L^2} N_{\text{f}}, \quad (2)$$

where p^{R} is the probability of two arbitrary fibers to intersect with each other in this case, l_{f} is the length of fiber, L is the length of squared representative area element (RAE), and the N_{f} is the number of fibers in this RAE. Detailed derivation of Eq.(2) can be found in the previous work. For the model with fiber aggregation, due to the non-single-level feature induced by aggregation, it is hard to obtain the average intersection number $\overline{N}_{\text{int}}$ by conventional geometric probability analysis, and thus a two-level analysis to calculate the average intersection number will be introduced in Section 2.2.

2.2. Analysis on the average intersection number

To analyze the average intersection number of fibers with aggregation, a two-level model based on the soft-core fiber network is set up first. Then the average intersecting probability between two fibers is derived based on the model.

2.2.1 Two-level aggregation model

As a widely used methodology, the aggregation model can be established based on the topological feature extracted from microscopy images of nanofiber composites with aggregation^{7, 16, 17}. According to the previous experimental and theoretical studies^{26, 28, 41}, the fibers in the composites usually aggregate into many aggregating clusters, and thus a two-level model^{7, 42} is built as follows. In the micro level of the aggregating cluster, the center points of the fibers follow a normal distribution in two perpendicular directions^{23, 42}, and the orientation angles of fibers follow uniform distributions in the ranges of $[0, \pi)$, as shown in Fig. 1 (a). Here σ is the standard deviation of normal distribution which characterizes the degree of looseness. The characteristic radius of the aggregating cluster is considered to be 3σ , which includes 99.7% of the fibers. In the macro level of the composites, there are multiple aggregating clusters distributing in the RAE with the size of $L \times L$, as shown in Fig.1 (b).

For simplicity, we assumed that all aggregating clusters in a RAE have the same degree of looseness σ and fiber number N_f^{agg} (other distribution laws will be discussed in Section 3). Thus the number of aggregating clusters in a RAE is

$$N^{\text{agg}} = \frac{N_f}{N_f^{\text{agg}}}. \quad (3)$$

In addition, when the fiber number in each aggregating cluster N_f^{agg} is 1, the aggregation model can degrade to the uniform distribution model. Besides, to evaluate the concentration of the fibers, the relative density is defined as the area fraction of the fibers in a RAE³⁸, as

$$\rho = \frac{N_f l_f d_f}{L^2} = \frac{n_f l_f^2}{\lambda_f}, \quad (4)$$

where d_f is the diameter of the fiber, $\lambda_f = l_f/d_f$ is the aspect ratio of the fiber, and $n_f = N_f/L^2$ is the number of fibers per unit area. For 2D networks, the diameter effect can be ignored if the aspect ratio is sufficiently large, and thus the combined dimensionless parameter $n_f l_f^2$, which is the average fiber number in the area of $l_f \times l_f$, also can be used to describe the density of fiber network.

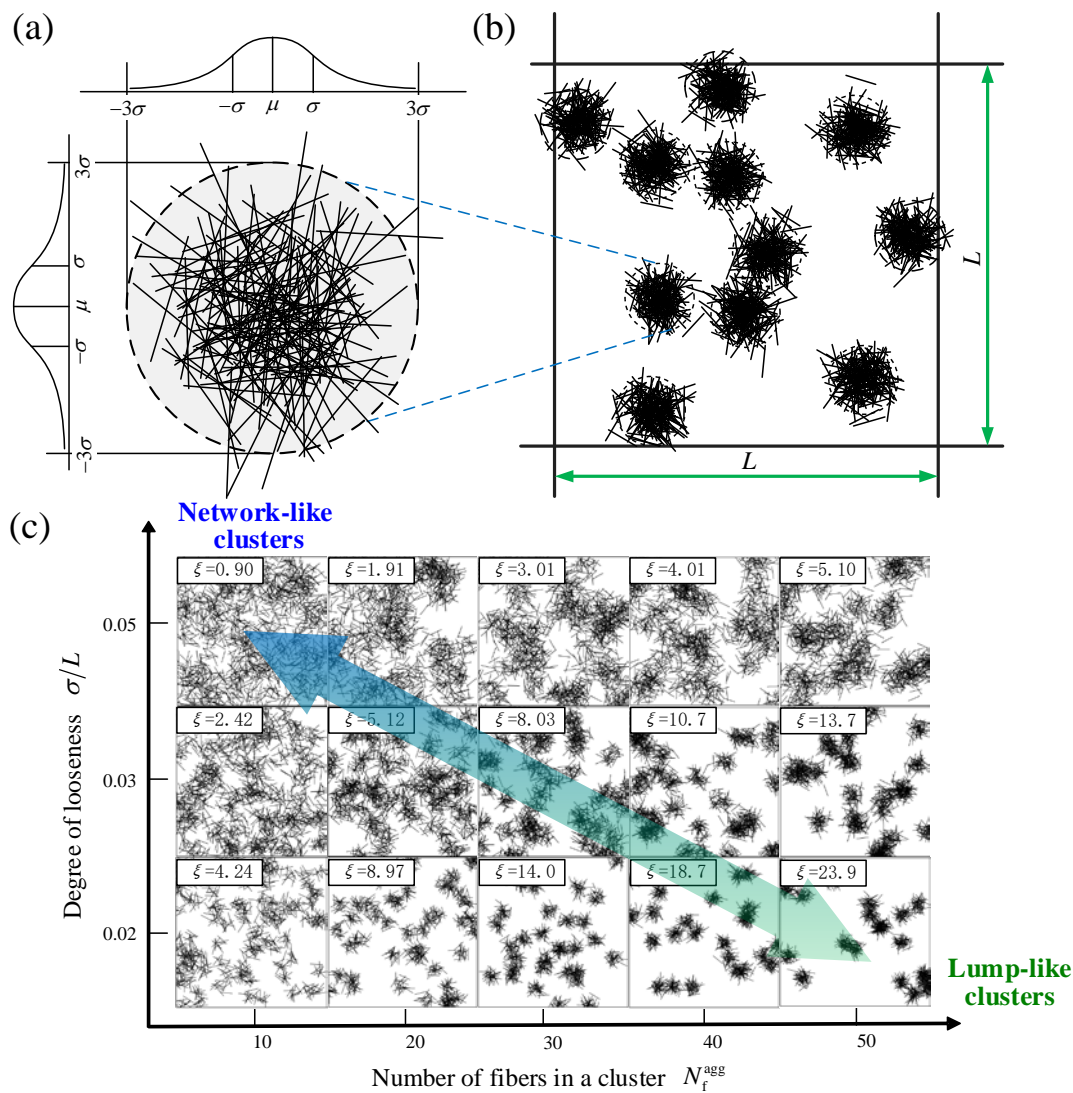


Fig. 1. Schematic

diagrams of (a) an aggregating cluster, (b) a RAE with multiple aggregating clusters, and (c) RAEs with different fiber dispersion states.

As shown in Fig. 1(c), RAEs with various dispersion states of fibers are exhibited. The aggregation degree ξ of each RAE is calculated by Eq.(1), as presented in the labels in Fig. 1(c). It can be seen intuitively that the fibers with stronger aggregation have a larger value of ξ . Meanwhile, it also can be found that the aggregation degree has the second feature, i.e., it applies to both lump-like clusters to network-like clusters.

2.2.2. Intersecting probability in an aggregating cluster

First, to calculate the intersecting probability of two arbitrary fibers in an individual aggregating cluster, a Cartesian coordinate system is introduced whose origin is located at the center of a characteristic circle, as shown in Fig. 2 (a). The intersecting probability of the two fibers depends on the distance R between the midpoints of the two fibers and the angle θ_{ij} between them. As the distance R decreases, or the angle θ_{ij} approaches to $\pi/2$, the intersecting probability increases. Based on geometric probability analysis, the intersecting probability of two fibers in an aggregating cluster is expressed as

$$p^{\text{agg}} = \iint G(R, \theta_{ij}) \cdot f(R) \cdot f(\theta_{ij}) dR d\theta_{ij}, \quad (5)$$

where $f(R)$ and $f(\theta_{ij})$ are the probability density functions of the distance R and angle θ_{ij} , respectively, and $G(R, \theta_{ij})$ is the intersecting probability of two fibers with given R and θ_{ij} . The details can be found in the Supplementary Information.

The intersecting probability of two fibers in an aggregating cluster p^{agg} can be obtained by Newton-Cotes numerical integration based on Eq.(5). By fitting the numerical results of Eq.(5), an approximate formulation of the intersecting probability in an aggregating cluster can be expressed as

$$p^{\text{agg}} \approx \frac{2}{\pi} \left[1 - \exp\left(-0.08(l_f/\sigma)^2\right) \right]. \quad (6)$$

To validate the theoretical result of Eq.(5) and the approximate solution of Eq.(6), Monte Carlo simulations³⁸ are used to obtain the intersecting probability of two fibers in an aggregating cluster. As shown in Fig. 2 (b), the numerical results from cases with different degree of looseness σ and the fiber length l_f fit well with the theoretical result of Eq.(5) and the approximate formulation in Eq.(6).

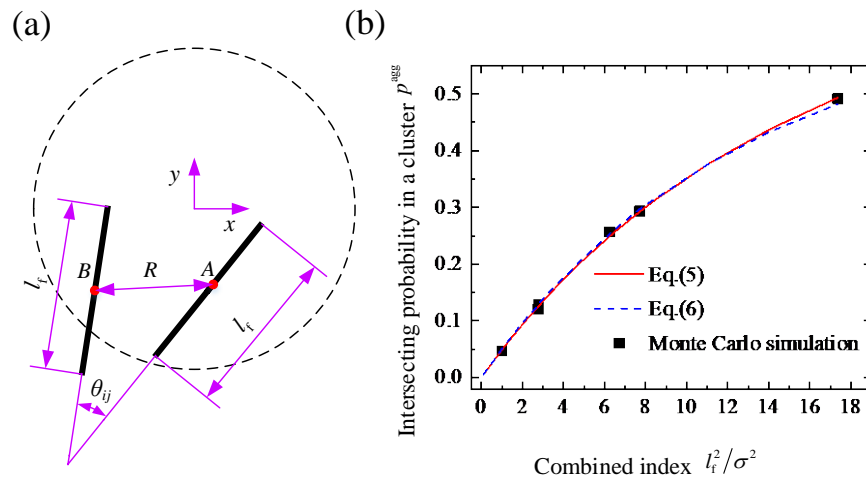


Fig. 2. (a) Schematic diagram of two arbitrary fibers in an aggregating cluster, and (b) the intersecting probability vs. combined index (l_f^2/σ^2).

2.2.3. Intersecting probability in a RAE

In this section, the intersecting probability of two fibers in a RAE is estimated. Obviously, the intersecting probability of two arbitrary fibers in a RAE p is a function of that in an aggregating cluster p^{agg} . To derive the relation between p and p^{agg} , a RAE with two aggregating clusters is taken as an introductory example first. The intersecting probability of two fibers in this RAE can be written as

$$p = \frac{2N_{\text{int}}}{N_f^2} = \frac{2p^{\text{agg}}(N_f^{\text{agg}})^2 + 2N_{\text{int}}^{\text{add}}}{(2N_f^{\text{agg}})^2}. \quad (7)$$

where N_{int} is the total number of intersections, $N_{\text{int}}^{\text{add}}$ is the number of intersections caused by intersecting fibers from two different aggregating clusters. Because the size of an aggregating cluster is typically much smaller than the RAE, the fibers from two different aggregating clusters can hardly intersect with each other. Therefore, the additional intersection number $N_{\text{int}}^{\text{add}}$ can be ignored compare to a much larger total intersection number N_{int} , and then the probability in Eq.(7) can be simplified as $p \approx p^{\text{agg}}/2$.

Therefore, it is intuitive that the intersecting probability must satisfy three special conditions, which are: (1) when $N^{\text{agg}} \rightarrow \infty$, $p \rightarrow p^{\text{R}}$; (2) when $N^{\text{agg}} \rightarrow 1$, $p \rightarrow p^{\text{agg}}/N^{\text{agg}}$; and (3) when $N^{\text{agg}}=1$, $p = p^{\text{agg}}$. Then the relation between p and p^{agg} is proposed as

$$p = \frac{p^{\text{agg}} - p^{\text{R}}}{N^{\text{agg}}} + p^{\text{R}}. \quad (8)$$

To validate the function in Eq.(8), Monte Carlo simulations are conducted by using RAEs with various parameters to numerically obtain the intersecting probability p . There are three parameters that affect the average intersecting probability, *i.e.*, the degree of looseness σ and the fiber length l_f , and the number of fibers in an aggregating cluster N_f^{agg} . Therefore, a comprehensive validation is summarized as shown in Fig. 3 (a), which shows a good agreement between the Monte Carlo simulation results and Eq.(8).

The average intersection number of each fiber in a RAE finally can be obtained as

$$\bar{N}_{\text{int}} = p \cdot N_f. \quad (9)$$

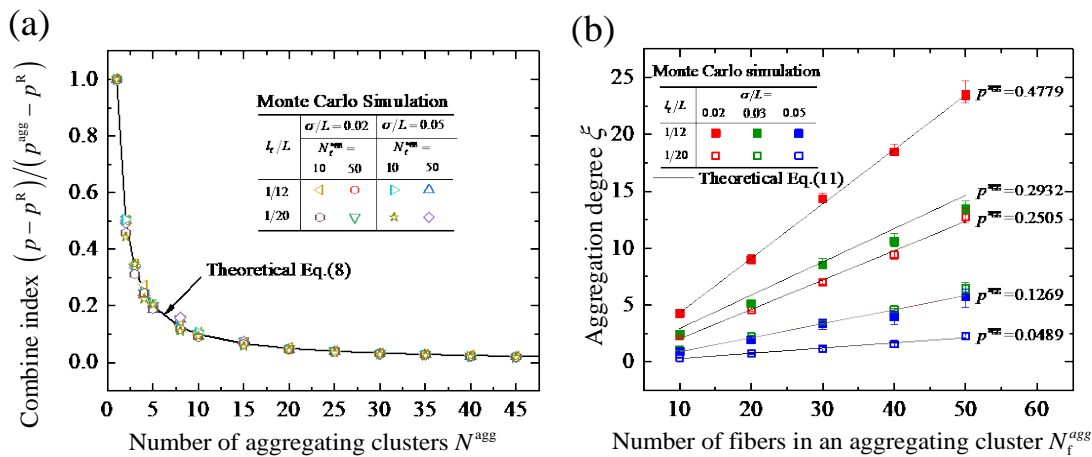


Fig. 3. (a) Validation of

the average intersecting probability, and (b) comparison between the aggregation degree obtained by theory and Monte Carlo simulation (error bars represent the maximum and minimum values of 80 different samples).

2.3. Results of the aggregation degree

Base on the analysis on the intersecting probability and the average intersection number, the aggregation degree of a RAE will be calculated in the following. According to Eqs.(1), (2), (3), (8) and (9), the aggregation degree can be expressed as

$$\xi = (p^{\text{agg}} - p^{\text{R}}) N_f^{\text{agg}}. \quad (10)$$

In general, the intersecting probability in aggregating cluster p^{agg} is much larger than that in composites with uniform distribution p^{R} , *i.e.* $p^{\text{agg}} \gg p^{\text{R}}$, thus Eq.(10) can be rewritten as

$$\xi = p^{\text{agg}} N_f^{\text{agg}} = \frac{2}{\pi} \left[1 - \exp\left(-0.08(l_f/\sigma)^2\right) \right] N_f^{\text{agg}}. \quad (11)$$

It can be seen from Eq.(11) that the aggregation degree is only dependent of the local features of aggregating cluster (σ and N_f^{agg}).

A comprehensive comparison between the theoretical results obtained by Eq.(11) and numerical results obtained by Eq.(1) using Monte Carlo simulations is shown in Fig. 3 (b). The theoretical results exhibit good consistency with the results of Monte Carlo simulations. Moreover, it should be noted that different fiber length l_f and degree of looseness σ may also have the same aggregation degree. (*e.g.* the cases when $p^{\text{agg}} = 0.1259$ in Fig. 3 (b)). The index provides a quantitative description of the degree of fiber aggregation, and can be used to qualify the performance of composites by combining quantitative evaluations of specific properties.

3. Linear relation between the aggregation degree and the percolation threshold

The aggregation degree has been proved to have the first and second features in Section 2. Then, does the aggregation degree have the third feature? *i.e.*, is there a one-to-one corresponding relation between the aggregation degree and percolation threshold regardless of the distribution law of fibers? In this section, the influence of the aggregation degree on percolation threshold is investigated accordingly.

The percolation threshold can also be obtained by Monte Carlo simulations^{8, 43-45}. In this study, a 2D soft-core fiber network model was used to predict the percolation threshold²², which has been proved to be in good agreement with experimental results⁴⁶. The two-level aggregation model proposed in the Section 2.2.1 was used. Percolation occurs when a connecting path that spans through the RAE is formed. Geometric (structural) percolation and electrical percolation are considered to occur simultaneously^{36, 37, 47}. Therefore, in the simulation, RAE samples of fiber networks were generated and then whether connecting paths are formed in each sample were checked. For a given set of parameters, the simulation can be repeated sufficiently large times (500 times in this work) to obtain a converged value of connection probability. With the increase of network density, an S-shaped sharp change from 0 to 100% can be captured for the connection probability, and the tendency can be well described by Boltzmann function. It has been proven that the network density when the connection probability is 50% can be used to estimate the percolation threshold. Besides, a RAE size of $L/l_f \geq 12$ is used to achieve numerical convergence²³. More details of the Monte Carlo simulation on the percolation threshold can be found in Appendix B.

Here the critical area fraction of fibers ρ_{th} to trigger the network connectivity, i.e., connection probability is 50%, is used to characterize the percolation threshold. For simplicity, a nominalized threshold $\hat{\rho}_{th}$ is defined as the ratio of the percolation threshold of aggregation model to that of uniformly distributed model ρ_{th}^R , as

$$\hat{\rho}_{th} = \frac{\rho_{th}}{\rho_{th}^R}. \quad (12)$$

where ρ_{th}^R is proven to be dependent on the aspect ratio of the fibers λ_f . For 2D model, it can be expressed as^{36,38}

$$\rho_{th}^R = \frac{5.8}{\lambda_f} = 5.8 \frac{d_f}{l_f}. \quad (13)$$

Fig. 4 (a) shows the relation between the aggregation degree and the percolation threshold. The normalized percolation threshold increases monotonically with the increase of the aggregation degree, which can be well linearly fitted as

$$\hat{\rho}_{th} = 0.12\xi + 1. \quad (14)$$

For fiber system with uniform distribution, i.e., the aggregation degree is 0, the corresponding normalized percolation threshold is 1. For fiber system with aggregation, the aggregation degree is greater than 0, and the aggregation degree increases with the degree of looseness σ and the number of fibers in an aggregating cluster N_f^{agg} . It is noted that although models with different parameters may have the same aggregation degree, the aggregation degree has a one-to-one corresponding relation with the threshold.

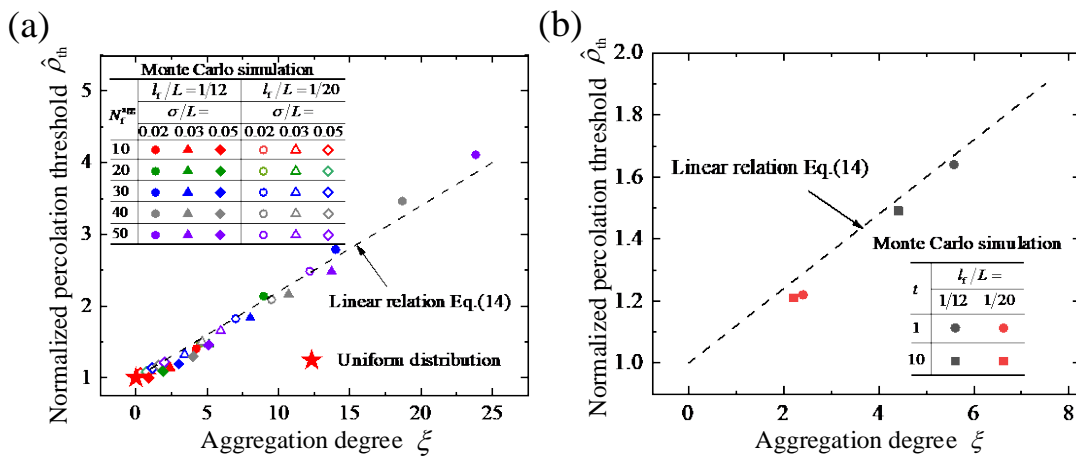


Fig. 4. (a) The relation

between the aggregation degree and the normalized percolation threshold, and (b) the relation between the aggregation degree and the normalized percolation threshold for fibers with different distributions.

The relation between the aggregation degree and the percolation threshold discussed above is based on the two-level model, where the randomly distributed aggregating clusters have the same size. However, in reality, the fibers

with aggregation may have different distributions, which rises another question: Is the linear corresponding relation still applicable to other fiber distributions? To answer this question, a distribution which is extracted from actual cases is built and discussed. In practice, the sizes of the aggregating clusters are diverse, and many studies have found that the frequency of aggregating clusters with different number of fibers follows a power law^{26, 28, 48}. This indicates that most aggregating clusters includes a small number of fibers, and aggregating clusters with larger number of fibers are much less. According to the previous studies^{26, 28}, the probability density of N_f^{agg} can be expressed as

$$f = C \left(N_f^{\text{agg}} \right)^{-t}, \quad (15)$$

where C is a constant, t is the exponent of the power law. It is assumed that the number of fibers in an aggregating cluster N_f^{agg} is proportional to the degree of looseness σ . Rejection sampling method⁴⁹ was then used to generate the fiber system with the power-law aggregation distribution. Here N_f^{agg} and σ are in the range of [10, 50] and [0.02, 0.05], respectively. Fig. 4 (b) shows the relation between the aggregation degree and the normalized percolation threshold of the models with power law slope $t = -1$ and -10 . The aggregation degree is calculated by Eq.(1). The results show that the linear relation of Eq.(14) is still applicable for the fiber system with power-law aggregation distribution. Therefore, it can be concluded that the proposed method in this work has well practicality and robustness, and the aggregation degree has the third feature.

For composites with aggregation degree ξ , the percolation threshold can be obtained from Eqs.(12), (13) and (14), and expressed as

$$\rho_{\text{th}}(\xi) = (0.696\xi + 5.8) \frac{d_f}{l_f}. \quad (16)$$

By virtue of this relation, the aggregation degree can be used to directly evaluation the properties in regard to percolation.

4. Conclusion

In this work, a simple and universal single index is proposed to characterize the dispersion state of fibers in nanocomposites, and the effect of fiber aggregation on the percolation threshold is studied by the proposed index. The following conclusions can be drawn.

The aggregation degree is defined as a dimensionless single index with a straightforward physical meaning. It is the increment of average intersection numbers of fibers in composites when fibers aggregate from a uniformly distributed state. Furthermore, based on a two-level model with randomly distributed aggregating clusters, we have demonstrated that the aggregation degree is applicable to different aggregation topologies from lump-like aggregating clusters to network-like aggregating clusters, and only depends on the local features of the aggregating clusters by both theoretical geometric probability analysis and Monte Carlo simulations. The index can be expressed as a combination of the intersecting probability and fiber numbers in an aggregating cluster.

A one-to-one relation between the aggregation degree and percolation threshold is established. By Monte Carlo simulations, the percolation threshold of composites with fiber aggregation is obtained. It is found that the percolation threshold increases monotonously with the increase of the aggregation degree, which can be fitted as a linear relation.

Furthermore, it is proven that this one-to-one linear relation between the aggregation degree and the percolation threshold is universally applicable to systems with different distribution laws.

The definition of the aggregation degree and its linear relation with the percolation threshold can not only provide a guide to the feature characterization, performance prediction and material design of nanocomposites, but also give a new physical insight into the understanding of system with complex randomness.

Data availability

All data used to generate these results is available in the main text or Supplementary Information. Further details could be obtained from the corresponding authors upon reasonable request.

Acknowledgements

Supports from the National Natural Science Foundation of China (Grant Nos. 12002016, 11472027 and 11622214), the National Postdoctoral Program for Innovative Talents in China (Grant No. BX20200032), the China Postdoctoral Science Foundation (Grant No. 2020M680288), and Beijing Advanced Discipline Center for Unmanned Aircraft System of China are gratefully acknowledged.

Appendix A. Supplementary information

Supplementary information to this article can be found in enclosure.

References

1. Samareh, J. A.; Siochi, E. J., Systems analysis of carbon nanotubes: opportunities and challenges for space applications. *Nanotechnology* **2017**, *28* (37), 372001.
2. Sun, W. J.; Xu, L.; Jia, L. C.; Zhou, C. G.; Li, Z. M., Highly conductive and stretchable carbon nanotube/thermoplastic polyurethane composite for wearable heater. *Compos. Sci. Technol.* **2019**, *181*, 107695.
3. Wu, Z. C.; Chen, Z. H.; Du, X.; Logan, J. M.; Sippel, J.; Nikolou, M.; Kamaras, K., Transparent, conductive carbon nanotube films. *Science* **2004**, *305* (5688), 1273-1276.
4. Hu, N.; Masuda, Z.; Yamamoto, G.; Fukunaga, H.; Hashida, T.; Qiu, J., Effect of fabrication process on electrical properties of polymer/multi-wall carbon nanotube nanocomposites. *Compos. Pt. A-Appl. Sci. Manuf.* **2008**, *39* (5), 893-903.
5. Shi, Y. D.; Li, J.; Tan, Y. J.; Chen, Y. F.; Wang, M., Percolation behavior of electromagnetic interference shielding in polymer/multi-walled carbon nanotube nanocomposites. *Compos. Sci. Technol.* **2019**, *170*, 70-76.
6. Kumar, S. D.; Ravichandran, M.; Alagarsamy, S.; Chanakyan, C.; Meignanamoorthy, M.;

Sakthivelu, S., Processing and properties of carbon nanotube reinforced composites: A review. *Materials Today: Proceedings* **2020**, *27*, 1152-1156.

7. Gong, S.; Zhu, Z. H.; Meguid, S. A., Carbon nanotube agglomeration effect on piezoresistivity of polymer nanocomposites. *Polymer* **2014**, *55* (21), 5488-5499.

8. Chen, Y.; Wang, S.; Pan, F.; Zhang, J., A Numerical Study on Electrical Percolation of Polymer-Matrix Composites with Hybrid Fillers of Carbon Nanotubes and Carbon Black. *J. Nanomater.* **2014**, (15), 1-9.

9. Zhang, M.; Lu, W.; Gouma, P. I.; Xu, Z.; Wang, L., Theoretical Prediction of Effective Stiffness of Nonwoven Fibrous Networks with Straight and Curved Nanofibers. *Compos. Pt. A-Apl. Sci. Manuf.* **2021**, (4), 106311.

10. Wang, S.; Lin, J.; Xu, Z.; Xu, Z., Understanding macroscopic assemblies of carbon nanostructures with microstructural complexity. *Compos. Pt. A-Apl. Sci. Manuf.* **2021**, *143* (5700), 106318.

11. Tang, Z.; Li, Y.; Huang, P.; Fu, Y.; Hu, N.; Fu, S., A new analytical model for predicting the electrical conductivity of carbon nanotube nanocomposites. *Compos. Commun.* **2021**, *23*, 100577.

12. Nanni, F.; Travaglia, P.; Valentini, M., Effect of carbon nanofibres dispersion on the microwave absorbing properties of CNF/epoxy composites. *Compos. Sci. Technol.* **2009**, *69* (3-4), 485-490.

13. Duc, B. N.; Son, Y., Enhanced dispersion of multi walled carbon nanotubes by an extensional batch mixer in polymer/MWCNT nanocomposites. *Compos. Commun.* **2020**, *21*, 100420.

14. Wang, Y.; Yang, C.; Xin, Z.; Luo, Y.; Wang, B.; Feng, X.; Mao, Z.; Sui, X., Poly(lactic acid)/carbon nanotube composites with enhanced electrical conductivity via a two-step dispersion strategy. *Compos. Commun.* **2022**, *30*, 101087.

15. Ma, P. C.; Siddiqui, N. A.; Marom, G.; Kim, J. K., Dispersion and functionalization of carbon

-
- nanotubes for polymer-based nanocomposites: A review. *Compos. Pt. A-Appl. Sci. Manuf.* **2010**, *41* (10), 1345-1367.
16. Ma, P. C.; Kim, J. K.; Tang, B. Z., Functionalization of carbon nanotubes using a silane coupling agent. *Carbon* **2006**, *44* (15), 3232-3238.
17. Haslam, M. D.; Raeymaekers, B., A composite index to quantify dispersion of carbon nanotubes in polymer-based composite materials. *Composites Part B: Engineering* **2013**, *55*, 16-21.
18. Jamali, S.; Paiva, M. C.; Covas, J. A., Dispersion and re-agglomeration phenomena during melt mixing of polypropylene with multi-wall carbon nanotubes. *Polym. Test* **2013**, *32* (4), 701–707.
19. Aguilar, J. O.; Bautista-Quijano, J. R.; Avilés, F., Influence of carbon nanotube clustering on the electrical conductivity of polymer composite films. *J. Appl. Phys.* **2010**, *4* (5), 292-299.
20. Kovacs, J. Z.; Velagalaa, B. S.; Schulteb, K.; Bauhofer, W., Two percolation thresholds in carbon nanotube epoxy composites. *Compos. Sci. Technol.* **2007**, *67* (5), 922-928.
21. Krause, B.; Poetschke, P.; Haeussler, L., Influence of small scale melt mixing conditions on electrical resistivity of carbon nanotube-polyamide composites. *Compos. Sci. Technol.* **2009**, *69* (10), 1505-1515.
22. Gbaguidi, A.; Namila, S.; Kim, D., Stochastic percolation model for the effect of nanotube agglomeration on the conductivity and piezoresistivity of hybrid nanocomposites. *Comput. Mater. Sci.* **2019**, *166*, 9-19.
23. Hu, N.; Masuda, Z.; Yan, C.; Yamamoto, G.; Fukunaga, H.; Hashida, T., The electrical properties of polymer nanocomposites with carbon nanotube fillers. *Nanotechnology* **2008**, *19* (21), 215701.
24. Matos, M. A. S.; Tagarielli, V. L.; Pinho, S. T., On the electrical conductivity of composites with a polymeric matrix and a non-uniform concentration of carbon nanotubes. *Compos. Sci. Technol.* **2020**, *188*,

108003.

25. Lv, Z.; Huang, X.; Fan, D.; Zhou, P.; Zhang, X., Scalable manufacturing of conductive rubber nanocomposites with ultralow percolation threshold for strain sensing applications. *Compos. Commun.* **2021**, *25*, 100685.
26. Fu, X.; Wang, J.; Ding, J.; Wu, H.; Dong, Y.; Fu, Y., Quantitative evaluation of carbon nanotube dispersion through scanning electron microscopy images. *Compos. Sci. Technol.* **2013**, *87*, 170-173.
27. Bakshi, S. R.; Agarwal, A., An analysis of the factors affecting strengthening in carbon nanotube reinforced aluminum composites. *Carbon* **2011**, *49* (2), 533-544.
28. Moon, D.; Obrzut, J.; Douglas, J. F.; Lam, T.; Koziol, K. K.; Migler, K. B., Three dimensional cluster distributions in processed multi-wall carbon nanotube polymer composites. *Polymer* **2014**, *55* (15), 3270-3277.
29. Yazdanbakhsh, A.; Grasley, Z.; Tyson, B.; Al-Rub, R. K. A., Dispersion quantification of inclusions in composites. *Compos. Pt. A-Appl. Sci. Manuf.* **2011**, *42* (1), 75-83.
30. Bakshi, S. R.; Batista, R. G.; Agarwal, A., Quantification of carbon nanotube distribution and property correlation in nanocomposites. *Compos. Pt. A-Appl. Sci. Manuf.* **2009**, *40* (8), 1311-1318.
31. Pfeifer, S.; Bandaru, P. R., A Methodology for Quantitatively Characterizing the Dispersion of Nanostructures in Polymers and Composites. *Mater. Res. Lett.* **2014**, *2* (3), 166-175.
32. Rohm, K.; Bonab, V. S.; Manas-Zloczower, I., Quantitative evaluation of mixing using a refined Shannon entropy. *Compos. Sci. Technol.* **2020**, 108276.
33. Sul, I. H.; Youn, J. R.; Song, Y. S., Quantitative dispersion evaluation of carbon nanotubes using a new analysis protocol. *Carbon* **2011**, *49* (4), 1473-1478.

-
34. Gong, S.; Zhu, Z. H.; Li, J.; Meguid, S. A., Modeling and characterization of carbon nanotube agglomeration effect on electrical conductivity of carbon nanotube polymer composites. *J. Appl. Phys.* **2014**, *116* (19), 305202.
 35. Alamusi; Hu, N.; Fukunaga, H.; Atobe, S.; Liu, Y.; Li, J., Piezoresistive strain sensors made from carbon nanotubes based polymer nanocomposites. *Sensors* **2011**, *11* (11), 10691-10723.
 36. Balberg, I.; Anderson, C.; Alexander, S.; Wagner, N., Excluded volume and its relation to the onset of percolation. *Phys. Rev. B* **1984**, *30* (7), 3933.
 37. Berhan, L.; Sastry, A. M., Modeling percolation in high-aspect-ratio fiber systems. I. Soft-core versus hard-core models. *Phys. Rev. E* **2007**, *75* (4), 041120.
 38. Chen, Y.; Fei, P.; Guo, Z.; Liu, B.; Zhang, J., Stiffness threshold of randomly distributed carbon nanotube networks. *J. Mech. Phys. Solids* **2015**, *84*, 395–423.
 39. Chen, Y.; Pan, F.; Wang, S.; Liu, B.; Zhang, J., Theoretical estimation on the percolation threshold for polymer matrix composites with hybrid fillers. *Compos. Struct.* **2015**, *124*, 292-299.
 40. Balberg, I.; Binenbaum, N.; Wagner, N., Percolation Thresholds in the Three-Dimensional Sticks System. *Phys. Rev. Lett.* **1984**, *52* (17), 1465-1468.
 41. Li, J.; Ma, P. C.; Chow, W. S.; To, C. K.; Tang, B. Z.; Kim, J. K., Correlations between percolation threshold, dispersion state, and aspect ratio of carbon nanotubes. *Adv. Funct. Mater.* **2007**, *17* (16), 3207-3215.
 42. Bao, W. S.; Meguid, S. A.; Zhu, Z. H.; Pan, Y.; Weng, G. J., A novel approach to predict the electrical conductivity of multifunctional nanocomposites. *Mech. Mater.* **2012**, *46*, 129-138.
 43. Pike, G.; Seager, C., Percolation and conductivity: A computer study. I. *Phys. Rev. B* **1974**, *10* (4), 1421.
 44. Kim, D. W.; Lim, J. H.; Yu, J., Efficient prediction of the electrical conductivity and percolation

threshold of nanocomposite containing spherical particles with three-dimensional random representative volume elements by random filler removal. *Composites Part B: Engineering* **2019**, *168*, 387-397.

45. Chang, E.; Ameli, A.; Alian, A. R.; Mark, L. H.; Yu, K.; Wang, S.; Park, C. B., Percolation mechanism and effective conductivity of mechanically deformed 3-dimensional composite networks: Computational modeling and experimental verification. *Compos. Pt. B-Eng.* **2021**, *207* (108552).

46. Theodosiou, T. C.; Saravanos, D. A., Numerical investigation of mechanisms affecting the piezoresistive properties of CNT-doped polymers using multi-scale models. *Compos. Sci. Technol.* **2010**, *70* (9), 1312-1320.

47. Jkw, S.; Kirk, J. E.; Kinloch, I. A.; Msp, S.; Windle, A. H., H.: Ultra-low electrical percolation threshold in carbon-nanotube-epoxy composites. *Polymer* **2003**, *44* (19), 5893-5899.

48. Tiwari, M.; Billing, B. K.; Bedi, H. S.; Agnihotri, P. K., Quantification of carbon nanotube dispersion and its correlation with mechanical and thermal properties of epoxy nanocomposites. *J. Appl. Polym. Sci.* **2020**, *137* (29).

49. Voss, J., *An introduction to statistical computing: a simulation-based approach*. John Wiley & Sons: 2013.